

Profiles of the normal and inverted semiconductor interfaces: A Zeeman study in asymmetric $\text{Cd}_{1-y}\text{Zn}_y\text{Te}/\text{CdTe}/\text{Cd}_{1-x}\text{Mn}_x\text{Te}$ quantum wells

W. Grieshaber, J. Cibert, J. A. Gaj,* Y. Merle d'Aubigné, and A. Wasiela

Laboratoire de Spectrométrie Physique, Université J. Fourier, Boîte Postale 87, 38402 Saint Martin d'Hères, France

(Received 1 April 1994)

The normal ($\text{Cd}_{1-x}\text{Mn}_x\text{Te}$ grown on CdTe) and inverted (CdTe on $\text{Cd}_{1-x}\text{Mn}_x\text{Te}$) interfaces are studied separately using a quantitative model of the Zeeman effect of excitons in asymmetric CdTe quantum wells with a magnetic $\text{Cd}_{1-x}\text{Mn}_x\text{Te}$ barrier on one side and a nonmagnetic $\text{Cd}_{1-y}\text{Zn}_y\text{Te}$ barrier on the opposite side. The extrinsic effect (dilution of Mn) is dominant at the inverted interface, while the normal interface allows a rather low upper bound to the intrinsic interface effect (due to missing nearest neighbors). Experimental results agree well with model profiles assuming a complete Cd/Mn exchange during growth between the surface layer and the subsurface layer.

Heterostructures incorporating diluted magnetic semiconductors are of considerable interest because it is possible, through the interaction between the carriers and the magnetic ions, to tune the band gap of the magnetic layers,¹ and hence the conduction- and valence-band offsets, by applying a magnetic field. When the structure is made of a nonmagnetic quantum well surrounded by magnetic barriers, as in a $\text{CdTe}/\text{Cd}_{1-x}\text{Mn}_x\text{Te}$ heterostructure, the magnetic field induces large changes of the confinement energies which are observed as large Zeeman effects of the excitons confined in the quantum well (QW). Results recently reported in the literature, particularly the impossibility of fitting the Zeeman effect measured in structures with various Mn concentrations with a single value of the band offset ratio,² has led some authors³ to suggest that in samples with high Mn content in the barrier the observed Zeeman splittings are in a large part due to interface effects. In bulk $\text{Cd}_{1-x}\text{Mn}_x\text{Te}$ with large x the magnetic susceptibility is strongly reduced due to antiferromagnetic exchange between nearest-neighbor Mn spins. The magnetism of Mn at the interface may be enhanced for two reasons. If the interface has a certain width because of interdiffusion or segregation the local concentration of Mn ions in this interface is smaller and thus their magnetic susceptibility larger (extrinsic effect). Even at a perfectly sharp interface the magnetization of the ion at the interface may be enhanced since the number of magnetic nearest neighbors is reduced, in a factor $\frac{2}{3}$ for a (001) interface ("surface-enhanced magnetism"). These interface effects are specially important in structures with large Mn content for two reasons: the barrier magnetic susceptibility is more severely reduced by antiferromagnetic exchange and the penetration of the carrier wave function in the barrier is reduced.

In this paper we present results on asymmetric $\text{Cd}_{1-x}\text{Mn}_x\text{Te}/\text{CdTe}/\text{Cd}_{1-y}\text{Zn}_y\text{Te}$ QW's which (i) demonstrate the importance of these interface effects, (ii) show that the normal interface ($\text{Cd}_{1-x}\text{Mn}_x\text{Te}$ on CdTe) is much sharper than the inverted one (CdTe on $\text{Cd}_{1-x}\text{Mn}_x\text{Te}$), and (iii) show that the extrinsic effect is generally much larger than the intrinsic surface-enhanced magnetism.

We describe Zeeman studies of a series of structures grown by pairs, the two members of a pair differing only by

the growth order of the magnetic ($\text{Cd}_{1-x}\text{Mn}_x\text{Te}$) and nonmagnetic ($\text{Cd}_{1-y}\text{Zn}_y\text{Te}$) barriers. Typical profiles are shown in Fig. 1. Figure 1(a) shows a structure in which the magnetic interface is "normal," $\text{Cd}_{1-x}\text{Mn}_x\text{Te}$ grown on CdTe , while Fig. 1(b) shows the "inverted" CdTe grown on $\text{Cd}_{1-x}\text{Mn}_x\text{Te}$ interface. In addition to the $\text{Cd}_{1-x}\text{Mn}_x\text{Te}$ and $\text{Cd}_{1-y}\text{Zn}_y\text{Te}$ barriers the structures contain buffer and cladding layers grown under the same conditions which allow an optical determination of barrier compositions. Thicknesses of layers were chosen below the critical thickness so that the structures are grown pseudomorphic on the $\text{Cd}_{0.88}\text{Zn}_{0.12}\text{Te}$ substrate. Structures differ essentially by the thicknesses L_w and L_{Mn} of the CdTe QW and of the $\text{Cd}_{1-x}\text{Mn}_x\text{Te}$ barrier. The thickness of the $\text{Cd}_{1-y}\text{Zn}_y\text{Te}$ barrier is constant, $L_{\text{Zn}} = 23$ ML (1 ML = 3.2 Å). Reflection high-energy electron diffraction (RHEED) oscillations were followed during all the growth and the thicknesses of the different layers are precisely known (Table I). Samples were grown at 280 °C under excess Cd, with a 2-min growth interruption in the vacuum at the interface before the first thin barrier, and a 20-s interruption at all other interfaces.

Reflectivity was measured with the sample immersed in liquid helium ($T = 1.7$ K). We observe both the e_1h_1 (between the first confined levels of electrons and heavy holes) and e_2h_2 excitons, and 3 meV below the e_1h_1 exciton line a relatively strong donor-related line.⁴ Photoluminescence (PL) was excited with an argon-ion laser. At low level of excitation, only the donor-related line is observed with a Stokes shift smaller than 0.2 meV. In both reflectivity and PL line widths are between 1.3 and 2 meV.

Zeeman shifts measured in σ^+ and σ^- polarizations for the pair $I3/N3$ are shown in Fig. 2. The Zeeman splitting is about four times larger for the inverted structure than for the normal one. As shown in Table I this is systematic. The two structures of a pair differ only by the growth order of the interfaces, hence (i) interface effects contribute strongly to the observed Zeeman splitting, (ii) the extrinsic effect is large at the inverted interface, and the normal magnetic interface is much "sharper" than the inverted one, (iii) the measure on the normal structures gives an upper bound of the contribution of the intrinsic surface magnetic effect; it is quite small.

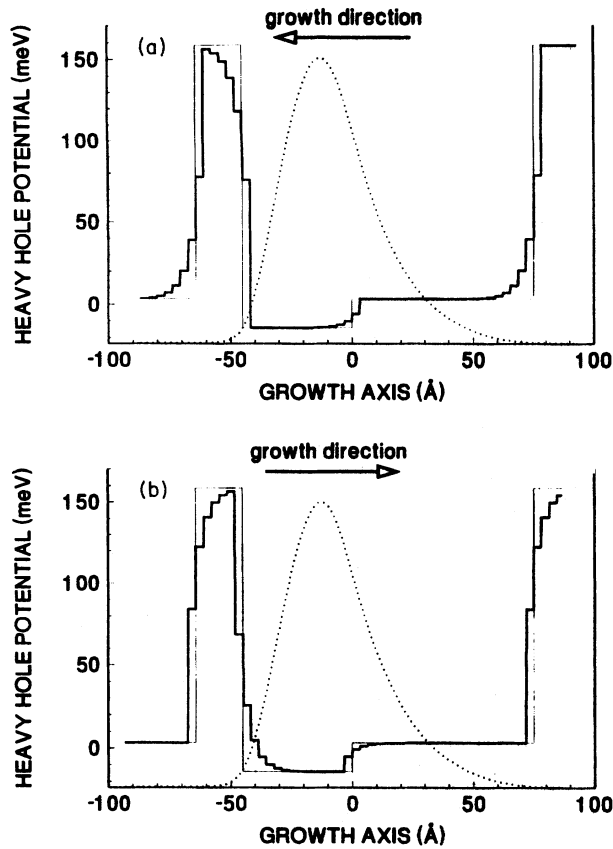


FIG. 1. Normal (a) and inverted (b) structures. Thin solid lines give the nominal potential profiles for heavy holes without magnetic field, thick lines give the exponential profiles obtained with $C=1$. The dotted lines show the squared amplitude of the hole wave function.

A quantitative analysis of the enhancement of the Zeeman splitting due to intermixing at the interface can be made using the model described previously.⁵ The model assumes an interface made of a laterally homogeneous alloy. The composition profile [represented by a function $x(z)$ where z is the growth axis] and the corresponding magnetization profile (obtained from Zeeman splitting on thick layers of uniform composition x) are combined to calculate potential profiles for electrons and holes with a given spin ($\pm \frac{1}{2}$ and $\pm \frac{3}{2}$, respectively). Then these potential profiles are used to calculate the carrier confinement energies. Making correction for exciton binding energies one calculates the exciton Zeeman shifts.

We used two interface profiles, a discrete quasiexponential one and a continuous error function one, corresponding to two different interface intermixing mechanisms.

Segregation at the surface of the growing layer produces an approximately exponential profile which is asymmetric relative to growth direction (Fig. 1): for the inverted interface the exponential tail of Mn concentration in the CdTe QW is at the origin of a large Zeeman effect while the steep initial raise of the exponential Mn profile in the normal interface explains the small observed Zeeman splitting. The profile was calculated as described in Ref. 6 assuming that exchange of Mn and Cd takes place only between the layer being grown and the one immediately below, and that the resultant concentrations x_s and x_i are given by the mass action law involving a phenomenological segregation energy E_s : $x_s(1-x_i)/x_i(1-x_s)=C=\exp(E_s/k_B T)$ where T is growth temperature. The important assumption to get the asymmetric profile is that exchange is limited to the near-surface layers. If $C=1$ we have no segregation, but still have exchange between surface layers.

The other limit is bulk-type interdiffusion, with a uniform diffusion coefficient. This mechanism may be eliminated since annealing experiments⁷ show that diffusion in

TABLE I. Sample parameters and experimental results. Thicknesses are deduced from RHEED oscillations, alloy compositions from reflectivity. To obtain the “measured exchange splitting” we subtract a direct Zeeman splitting (-0.3 meV) from the experimental one. Model parameters are fitted for C on inverted structures with the same value of C on all interfaces, for l_{inv} on inverted structures taking $l_{nor}=2.5$ Å on the normal interface (fit not sensitive to the exact value of l_{nor}) and for l_{nor} on normal structures taking $l_{inv}=7.2$ Å (fit not very sensitive to l_{inv} , but may be sensitive to direct Zeeman effect).

Sample	Inverted growth direction				Normal growth direction			
	I1	I2	I3	I4	N1	N2	N3	N4
L_w (Å)	47.0	46.7	50.9	67.8	44.2	43.2	53.8	69.8
L_{Mn} (Å)	11.2	19.4	25.6	25.6	11.2	19.4	25.6	25.6
y (%)	11.2	11.2	14.3	14.0	11.3	11.7	14.2	14.1
x (%)	33.9	35.1	38.8	37.9	32.3	32.0	37.5	38.5
Measured exchange splitting (meV) at 5 T	4.5	4.3	4.6	2.8	2.3	1.7	1.4	0.8
Fitted C	0.92 ± 0.08	1.01 ± 0.07	1.05 ± 0.07	1.08 ± 0.11				
Calculated exchange splitting (meV) with $C=1$	4.8	4.3	4.4	2.6	2.1	1.7	1.0	0.5
Fitted l_{inv} (Å)	6.1 ± 0.3	6.9 ± 0.3	$7.5^{+0.3}_{-0.4}$	$7.9^{+0.5}_{-0.6}$				
Fitted l_{nor} (Å)					$2.4^{+0.5}_{-0.6}$	2.2 ± 0.6	$3.2^{+0.6}_{-0.7}$	$3.2^{+0.9}_{-0.8}$
Calculated exchange splitting (meV) with $l_{inv}=7.2$ Å and $l_{nor}=2.5$ Å	5.6	4.3	4.4	2.5	2.3	1.8	1.1	0.6

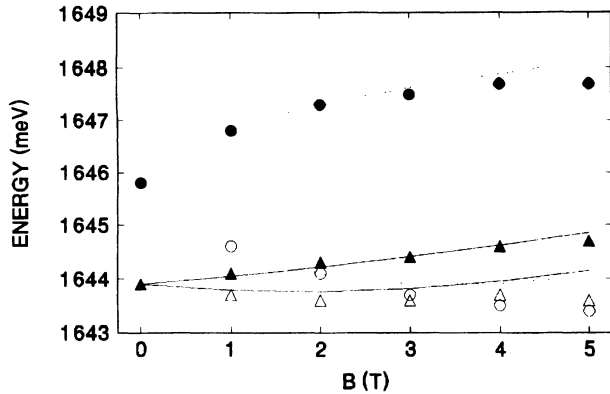


FIG. 2. Energy of the e_1h_1 exciton lines for a pair of structures: triangles, measured on the normal structure (sample $N3$); circles, measured on the inverted structure (sample $I3$). Open symbols are for σ^+ polarization, closed symbols for σ^- . Calculated shifts (exponential profile, $C=1$) are given by dotted (sample $I3$) and solid lines (sample $N3$).

$\text{CdTe}/\text{Cd}_{1-x}\text{Mn}_x\text{Te}$ QW's starts at temperatures higher than the growth temperature used (280°C). Moreover bulk-type interdiffusion leads to a symmetrical QW profile with identical interfaces. However, short-scale surface roughness developed during the growth of the $\text{Cd}_{1-x}\text{Mn}_x\text{Te}$, Mn depletion at the $\text{Cd}_{1-x}\text{Mn}_x\text{Te}$ surface, etc., are among other possible mechanisms which we tentatively describe with two different continuous error functions at the inverted and direct interfaces.

The intrinsic surface magnetic effect is estimated using the crude model described in Ref. 8. Due to the reduction of the number of magnetic neighbors the magnetization of a given Mn ion at the interface is enhanced relative to its value in a bulk crystal with the same composition $x(z)$. We assume that it is equal to the magnetization per ion in an alloy of composition $x_{\text{eff}}(z)=[x(z)+x(z+a)+x(z-a)]/3$, i.e., an alloy with the same average number of magnetic nearest neighbors ($a=1$ ML). The extreme situation is obtained for an atomic plane of $\text{Cd}_{1-x}\text{Mn}_x\text{Te}$ embedded between two nonmagnetic CdTe or $\text{Cd}_{1-y}\text{Zn}_y\text{Te}$ layers. Then the number of magnetic nearest neighbors is reduced by a factor 3 and the effect of antiferromagnetic exchange between the Mn spins is strongly reduced. Such structures will be described in a future publication. In the present study the $\text{Cd}_{1-x}\text{Mn}_x\text{Te}$ thickness L_{Mn} was kept larger than 3.5 ML, so that the two interfaces of the $\text{Cd}_{1-x}\text{Mn}_x\text{Te}$ barriers are well separated, and, as will be seen, the intrinsic effect is only a weak correction at the inverted interface but becomes significant at the normal interface.

Beside the exchange mediated $\sigma^- - \sigma^+$ Zeeman splitting we always have direct influence of the magnetic field on the carriers spin producing the usual "direct" spin splitting. Measurements made on $\text{Cd}_{1-y}\text{Zn}_y\text{Te}-\text{CdTe}$ QW's show that this splitting depends on the QW width, barrier height, and strain, and that at 5 T it ranges between 0 and -0.6 meV. It has the opposite sign to the exchange mediated one. In Table I we have reported the exchange mediated splitting at 5 T, which we take as the sum of the absolute values of the measured splitting and of an estimated direct Zeeman effect (-0.3 meV at 5 T).

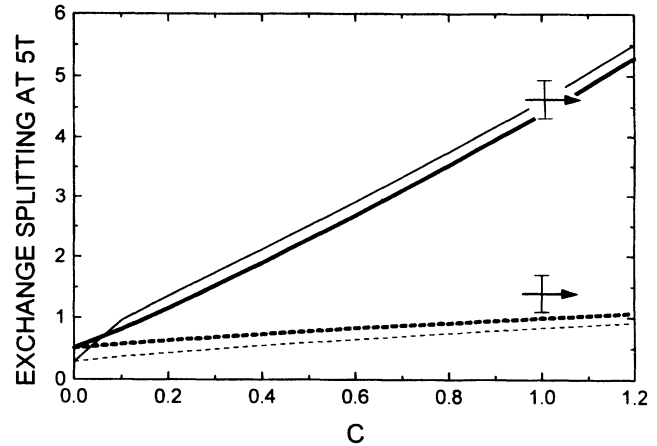


FIG. 3. Exchange Zeeman splitting at 5 T calculated for samples $I3$ (solid lines) and $N3$ (dotted lines), as a function of the segregation coefficient C , taking into account (thick lines) or neglecting (thin lines) the intrinsic "surface-enhanced magnetism." Arrows are experimental findings with "error bars" corresponding to the estimated direct Zeeman effect.

Simulations are made using as effective masses $m_e^*=0.096m_0$, $m_h^*=0.51m_0$, and a relative valence band offset $\alpha=0.3$; we checked that the conclusions depend little on these values.

The result of the simulations is shown in Table I. For the exponential profile we assume the same equilibrium model for all the $\text{CdTe}-\text{Cd}_{1-x}\text{Mn}_x\text{Te}$ and $\text{CdTe}-\text{Cd}_{1-y}\text{Zn}_y\text{Te}$ interfaces; thus we have only one adjustable parameter. All the inverted structures are well fitted with the value $C=1\pm 0.2$. This means a total exchange between the layer being grown and the one immediately below. Then the profile is exponential with a characteristic length $l_s=1/\ln(2)\approx 1.4$ ML. The uncertainty in the value of C and of l_s (generally ± 0.2 Å) results from the uncertainty in the direct Zeeman effect (0.3 meV at 5 T).

For normal structures the measured splittings are small. Then the uncertainty on the exact value of the "direct" Zeeman contribution and the crudeness of the description of the intrinsic surface effect make a determination of the intermixing range doubtful. It is thus remarkable that one obtains a good fit using $C=1$ as determined on the inverted structures. From these data on normal structures one deduces that for sharp interfaces the intrinsic surface magnetic effect contributes by at most 0.4 meV to the splitting at 5 T. Thus it is a small fraction of the splitting measured in inverted structures. On the other hand, the estimation using our crude model shows that it can be significant at the normal interface.

Figure 3 shows the sensitivity of the determination of intermixing in the case of the normal and inverted structures. The exchange-mediated splitting is plotted as a function of C . Thick and thin lines, respectively, include and omit the correction for intrinsic surface magnetism. It is seen that this correction is important only at very small intermixing range. Arrows give the experimental results, with error bars corresponding to the contribution of the direct Zeeman splitting (0 to -0.6 meV): it influences little our determination of C using the inverted structure.

Using now error function profiles, we define two lengths

l_{inv} and l_{nor} which are the width of the error function (15–85 % at $\pm l$) for the inverted and for the normal interface, respectively. Calculations show that, for samples with $L_{\text{Mn}} \geq 3.5$ ML, the exchange-mediated splitting of the inverted structure varies quickly with l_{inv} and very little with l_{nor} , and the splitting on the normal structure varies quickly with l_{nor} and little with l_{inv} . Thus the two parameters can be considered as determined independently. For the final fit given in Table I we determined l_{inv} assuming $l_{\text{nor}} = 2.5$ Å and l_{nor} assuming $l_{\text{inv}} = 7.2$ Å. The uncertainty on the values of l_{nor} are large (of the order of 50%) because of the relatively large contribution of the direct Zeeman effect to the measured splitting.

From the present analysis we do not have strong arguments to decide between the two profiles which both allow a good description of the experimental results. Transmission electron microscopy measurements on MnTe layers embedded in CdTe (Ref. 9) show a larger width for the inverted interface than for the normal one. This width increases with the MnTe layer thickness as expected if it originates from roughness developing during the growth of MnTe, an assumption consistent with the fact that the growth of MnTe was realized at a temperature too low for RHEED oscilla-

tions to be observed. On the other hand, RHEED oscillations were observed during the growth of the present structures and we notice no increase of the characteristic length l_{inv} in the inverted structures when the thickness L_{Mn} of the $\text{Cd}_{1-x}\text{Mn}_x\text{Te}$ barrier varies from 3.5 to 8 ML (Table I). We may attribute the increasing roughness of the MnTe surface to a too low surface diffusion of the Mn adatoms, while in the case of $\text{Cd}_{1-x}\text{Mn}_x\text{Te}$ the surface diffusion of the Cd adatoms is large enough to smooth the surface. Thus a mechanism with local diffusion leading to an exponential profile which allows us to fit all the experimental results with a single adjustable parameter looks more probable. The value we determine for the “segregation” coefficient, $C = 1$, implies a complete exchange between the first two surface layers and does not lead to segregation in the usual meaning. We may note, even if the conditions are very different, that a segregation coefficient close to unity is also observed in the Bridgman growth of $\text{Cd}_{1-x}\text{Mn}_x\text{Te}$.¹⁰

We acknowledge discussions with R. Planel (L2M-Bagneux, France) who suggested the study of asymmetric structures. This work was completed within the CNRS-CEA joined group “Microstructures de Semiconducteurs II-VI.”

*On leave from Warsaw University, Warsaw, Poland.

¹A review paper is J. K. Furdyna, *J. Appl. Phys.* **64**, R29 (1988).

²B. Kuhn-Heinrich, W. Ossau, M. Popp, E. Bangert, A. Waag, and G. Landwehr, in *Proceedings of the International Conference on The Physics of Semiconductors, Beijing, 1992*, edited by Ping Jiang and Hou-Zhi Zheng (World Scientific, Singapore, 1993), p. 923.

³S. K. Chang, D. Lee, H. Nakata, A. V. Nurmikko, L. A. Kolodzielski, and R. L. Gunshor, *J. Appl. Phys.* **62**, 4835 (1987); A. Wasiela, Y. Merle d’Aubigné, J. E. Nicholls, D. E. Ashenford, and B. Lunn, *Solid State Commun.* **76**, 263 (1990).

⁴K. Kheng, R. T. Cox, Y. Merle d’Aubigné, F. Bassani, K. Saminadayar, and S. Tatarenko, *Phys. Rev. Lett.* **71**, 1752 (1993).

⁵J. A. Gaj, C. Bodin-Deshayes, P. Peyla, J. Cibert, G. Feuillet, Y. Merle d’Aubigné, R. Romestain, and A. Wasiela, in *Proceedings*

of the International Conference on The Physics of Semiconductors, Beijing, 1992 (Ref. 2), p. 1936.

⁶J. M. Moison, C. Guille, F. Houzay, F. Barthe, and M. Van Rompay, *Phys. Rev. B* **40**, 6149 (1989).

⁷D. Tönnies, G. Bacher, A. Forchel, A. Waag, Th. Litz, D. Hommel, Ch. Becker, G. Landwehr, M. Heuken, and M. Scholl, *International Conference on II-VI Semiconductors, Newport, 1993* [*J. Cryst. Growth* (to be published)].

⁸J. A. Gaj, W. Grieshaber, C. Bodin-Deshayes, J. Cibert, G. Feuillet, Y. Merle d’Aubigné, and A. Wasiela, *Phys. Rev. B* (to be published).

⁹P. H. Jouneau, A. Tardot, G. Feuillet, H. Mariette, and J. Cibert, *J. Appl. Phys.* (to be published).

¹⁰R. Triboulet and G. Didier, *J. Cryst. Growth* **52**, 614 (1981).